Applied GIS

ISSN: 1832-5505
Vol-2 Issue-01 Jan 2014

Buildings on the Flood Plains of the Santo Tomas River Basin, Zambales, Philippines: An Exposure and Vulnerability Assessment Utilizing LiDAR Derived Datasets

Annie Melinda Paz-Alberto[1], Gloria N. Ramos[1], Hanna Mae T. Carganilla[1], Cenon Conrado C. Divina[1], Jeremy Joel J. Barza[1]

Abstract

Because of its tropical location, the Philippines is often struck by monsoons and typhoons. Flooding caused by typhoons poses a significant threat to human life and property because of the rapid accumulation of water. This research combined and addressed the use of the catastrophe risk management techniques of Light Detection and Ranging (LiDAR) with a Geographic Information System (GIS). Based on GIS overlay analysis using the CLSU PHIL-LiDAR 1 Project outputs, the 3D building GIS database, and flood hazard maps, this article maps and assesses exposure of structures and susceptibility to floods in the Santo Tomas River Basin in Zambales, Philippines. The 3D building GIS database was compiled by analyzing several datasets, such as geo-tagged video footage and high-resolution photos of Google Earth, as well as 1m-resolution LiDAR Digital Elevation Models (DEMs). Flood models were created using the combined HEC HMS and HEC RAS, which allowed for the generation of flood hazard maps with varying degrees of danger. This research produced a set of flood risk and exposure maps based on statistical analysis of various precipitation scenarios. At the 100-year return period, the number of exposed and endangered structures is greatest. There were a total of 42,173 building characteristics collected, with 24,738 buildings at low risk, 12,670 at medium risk, and 4,620 at high risk throughout the 100-year return period. In terms of building height and flood risk at low, medium, and high levels of danger, a total of 8,938 buildings, 12,259 structures, and 4,556 buildings were found. When it comes to managing flood disasters and preparing for them, these maps may be invaluable resources for local government entities and communities in the Santo Tomas river basin.

Keywords: *LiDAR, Geographic Information System, Flood, Database, Extraction & Hazard.*

1. Introduction

1.1. Background of the Study

Flooding is a serious and costly hazard that the Philippines faces regularly during monsoon and typhoon occurrences. Flood is defined as extremely high flows or levels of rivers, lakes, ponds, reservoirs and any other water bodies, whereby water inundates

ISSN: 1832-5505
Vol-2 Issue-01 Jan 2014

outside the water body area (Tambunan, 2007). Flooding also occurs when the sea level raises extremely or above coastal lands due to tidal sea and sea surges. In many regions and countries, floods are the most damaging phenomena that effect to the social and economic aspects of a certain area (Smith et, al., 1998). Due to excessive rainfall in a short period of time caused by natural phenomenon, flooding is a frequent hazard in the flood plains of Santo Tomas River that cause tremendous losses in terms of property and life.

Many flood plains have been occupied by residential areas and industrial parks during the last few decades. In some cases, nearby rivers have been confined in narrow strips by embankments, and cheap and attractive land has been reclaimed. Towns and village areas have been declared as residential areas and, therefore, many potential buyers of property were assured that no flood hazards are to be feared (Kron, 2005). The identification and mapping of flood prone areas are essential for risk reduction. The flood hazard maps display flood hazard information in a given area which can be used in area development and management planning. In the twenty-first century the need to study both exposure and vulnerability as fundamental components of risks has been heightened by the International Strategy for Disaster Reduction, supported by a new focus directed towards the disaster reduction through effective risk management. In the Hyogo Action Framework 2005 to 2015, governments from the whole world were certain to take measures in reducing exposure and vulnerability to natural threats (UNISDR, 2005).

Exposure can be defined as the assets and values located in flood-prone areas (IPCC, 2012). Together, exposure refers to the location of people or economic and social assets in hazard-prone areas subject to potential losses. They are also commonly referred to as “elements at risk”. Vulnerability characterizes the circumstances of a community, system or tangible assets that make the subject susceptible to damage and losses from a hazard (UNISDR, 2011b).

As topography is one of the major factors in most types of hazard analysis, the LiDAR data have become a major source of digital terrain information (Raber et al., 2007). LiDAR is a remote sensing technology characterized by precise vertical and horizontal point accuracy (Yunfei, 2008) and is significant for several applications that includes the generation of Digital Terrain Models (DEM) and Digital Surface Models (DSM) and building footprint extraction (Ruijin, 2005). With the existing modern LiDAR technology integrated with some forms of field data within GIS boundary, a better visualization of interactive map overlays quickly illustrate which areas of a community are in hazard of flooding. Such maps can then be used to coordinate mitigation efforts before an event and recovery after the event (Noah Raford, 1999 as cited in Awal, 2003).

In this study, the mapping and assessment of buildings exposed and vulnerable to flood in the flood plains of Santo Tomas river basin in Zambales was conducted and the generation of the 3D building GIS database that was used for the assessments was also presented. The assessments was done through GIS overlay analysis using the CLSU PHIL-LiDAR 1 Project flood hazard maps outputs and generated 3D building GIS database. This study focuses on identifying the number of buildings exposed to different flood hazard depth at varying rainfall return periods.

The general objective of the study was to generate a 3D Building GIS database and

ISSN: 1832-5505
Vol-2 Issue-01 Jan 2014

determine the exposure and vulnerability of buildings (in terms of height) to flood hazard at varying rainfall return periods in Santo Tomas River basin. Specifically, this study aimed to:

- generate a 3D building GIS database for the Santo Tomas River flood plains.
- map the buildings exposure and vulnerability to flood hazard in Santo Tomas River's basin using GIS
- assess the exposure and vulnerability of buildings to flood at different rainfall scenarios with varying intensity and duration.

2. Materials and Methods

2.1. The Study Area

Santo Tomas River is located in the Province of Zambales, Central Luzon, Philippines (Figure 1). Santo Tomas river basin has a total area of 261.22 km^2 with an approximately 313.53-km^2 flood plain area. Santo Tomas River is a joined larger river of Marella and Mapanuepe Rivers with the Mapanuepe lake as confluence. The watershed is located in the southern part of the province of Zambales. Bounded on the North by municipalities of Botolan and San Felipe; on the South by municipalities of Subic, Castillejos and San Marcelino: on the West by South China Sea/Philippine Sea: and on the East by Mount Dutdut bordering the province of Pampanga (DENR, 2008). The 6 municipalities in the Province of Zambales were covered by the flood plain area of Santo Tomas river basin. These municipalities are the Municipality of San Felipe, San Antonio, San Narciso (at the lowest portion of the river), San Marcelino, Castillejos (at the upper portion of the river) and partly of the municipality of Subic. The 235-km^{2}alluvial plain below the junction is populated by some 140,000 inhabitants in five municipalities, each with numerous *barangays* and *sitios* (Umbal and Rodolfo, 1992).

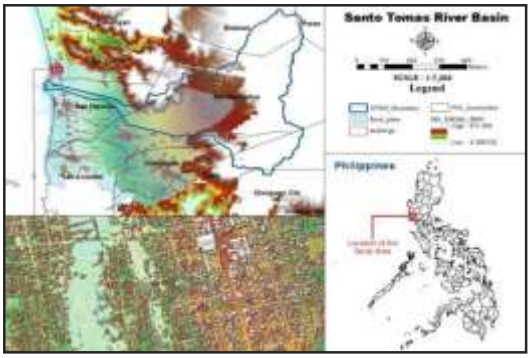

Figure 1: The Santo Tomas River Basin in Zambales, Philippines.

2.2. Datasets used

The LiDAR derived Digital Surface Model (DSM) and Digital Terrain Model (DTM) with 1-m resolution acquired and processed by UPD PHIL-LiDAR 1 project were used for the extraction of building footprints in the flood plains of Santo Tomas River basin. These Digital Elevation Models (DEMs) have the Mean Sea Level as vertical datum and were delivered in ESRI GRID format with Universal Transverse Mercator (UTM) Zone 51 North projection and the World Geodetic System (WGS) 1984 as horizontal reference. For improved accuracy in building footprints extraction, Google Earth images were utilized in rechecking of the existence and shapes of the extracted features from LiDAR DSM where in the created fishnet of rectangular cells was overlaid and served as a guide in both building footprint extraction and existence rechecking in Google Earth. Extracted building features were also verified and field validated with the use of video-tagging device or geo tagged video capturing tool where in information's such as name and type were gathered. Geo Tagged Video Capture Tool, or Mio MiVue 128, is a compact digital video recorder with built-in highly sensitive GPS receiver and the all-in-one Mio Manager PC suite. This device is

ISSN: 1832-5505
Vol-2 Issue-01 Jan 2014

available on the commercial market allowing easy installation and can be used as a tool in building assessment. It uses Micro SD card with a maximum capacity of 32GB that can save quality videos up to 8 hours. The recorder simultaneously records the video and the other info like locations, directions, speed and coordinates. This allows users to easily and accurately correlate video imagery with geographic location and other travel information. The table from UPD PHIL-LiDAR 1 project contains a summary of different types of buildings with corresponding codes for the building type attribute.

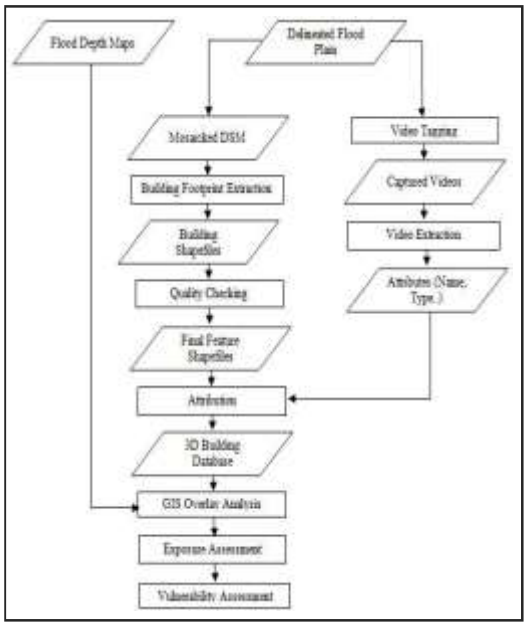

Figure 2: The work flow.

The flood depth maps generated by Central Luzon State University (CLSU) PHIL-LiDAR1 project were used as input in assessing flood exposure and the vulnerability. These flood depth maps represent maximum depth of flooding due to rainfall events with varying intensity and duration (i.e., return period of 5, 25 and 100-year). Flood depth maps were transformed into flood hazard maps by categorizing the flood depths in hazard levels as follows: low (< 0.5m depth), medium (0.5 - 1.5 m) and high (> 1.5 m). In order to determine the reliability and accuracy of the generated flood depth maps to the observed flood depths in the area, field validation was conducted. Based on the results of the data from the field, the models had indicated a positive bias with an RMSE value of 0.84 which signifies that the generated flood hazard maps can produce reliable information about exposure and vulnerability assessment. Figure 2 shows the work flow of the research work.

2.3. Generation of Building GIS Database

2.3.1. Building Features Extraction

For a more accurate number of buildings in the study area, features were manually digitized where footprints were traced by the polygon feature type from the LiDAR Digital Surface Model using ArcGIS 10.2 software. The existence and shape of the extracted buildings were checked using the corresponding high resolution Google Earth images due to the reason that some buildings and their extents were indistinguishable in the DSM.

2.3.2. Building Features Attribution

All building features extracted were attributed following the various building types as shown in Table 1. With the use of the integrated Spatial Analyst in GIS, automated buildings height extraction from normalized Digital Surface Model (NDSM) was performed. The normalized DSM represents the height of the object from the terrain which was produced with the difference between Digital Surface Model (DSM) and Digital Terrain Model (DTM). The building height ranges considered are greater than or equal to 2-m. Therefore, digitized buildings with height of less than 2m were deleted. This assumes that only those features which are having the said height are considered as buildings.

ISSN: 1832-5505
Vol-2 Issue-01 Jan 2014

Table 1: Building types with corresponding codes that were used in the buildings attribution (UP-PHIL-LiDAR).

Building Type	Code
Residential	RS
School	SC
Market/Prominent Stores	MK
Agricultural & Agro-Industrial	AG
Medical Institution	MD
Barangay Hall	BH
Military Institution	ML
Sports Center/Gymnasium/Covered Court	SP
Telecommunication Facilities	TC
Transport Terminal (Road, Rail, Air, and Marine)	TR
Warehouse	WH
Power Plant/Substation	PP
NGO/CSO Offices	NG
Police Station	PO
Water Supply/Sewerage	WT
Religious Institution	RL
Bank	BN
Factory	FC
Gas Station	GS
Fire Station	FR
Other Government Offices	OG
Other Commercial Establishments	OC

The name and type of the buildings were extracted and collected in the captured video by conducting building survey using video tagging device. During the survey, two video capture tools were attached to the windshield of a car using a mounting frame with one attached on the left side and the other on the right side of the car to collect the building characteristics and building location. Printed maps of the area being surveyed were also used for a planned and monitored path. The field survey conducted and the sample video captured in the Municipality of San Felipe, Zambales, Philippines is presented in Figure 3.

Figure 3: The field survey conducted and the snapshots of the captured video in Santo Tomas River flood plains.

2.4. Generation of Flood Hazard Maps

Through the CLSU PHIL-LiDAR 1 project, Flood depth maps were generated and used as input in flood exposure of buildings exposure and vulnerability assessment in the flood plains of Santo Tomas River basin. The flood depth maps were generated through the use of the flood model of the river basin from the combined HEC HMS hydrological model and HEC RAS hydraulic model. The flood depth maps represent maximum depth of flooding due to rainfall events with varying return periods (5, 25, and 100-year return periods) where the discharges or flow data inputs were the computed 5, 25 and 100-year return period of rainfall events in the Santo Tomas river watershed. These flood depth maps were transformed into flood hazard maps by

ISSN: 1832-5505
Vol-2 Issue-01 Jan 2014

categorizing the flood depths into hazard levels as low (<0.50 m depth), medium (0.50 m – 1.50 m depth), and high (>1.5 m depth). Figure 4 illustrates the Santo Tomas flood hazard maps at 5-year, 25-year and 100-year return period, respectively.

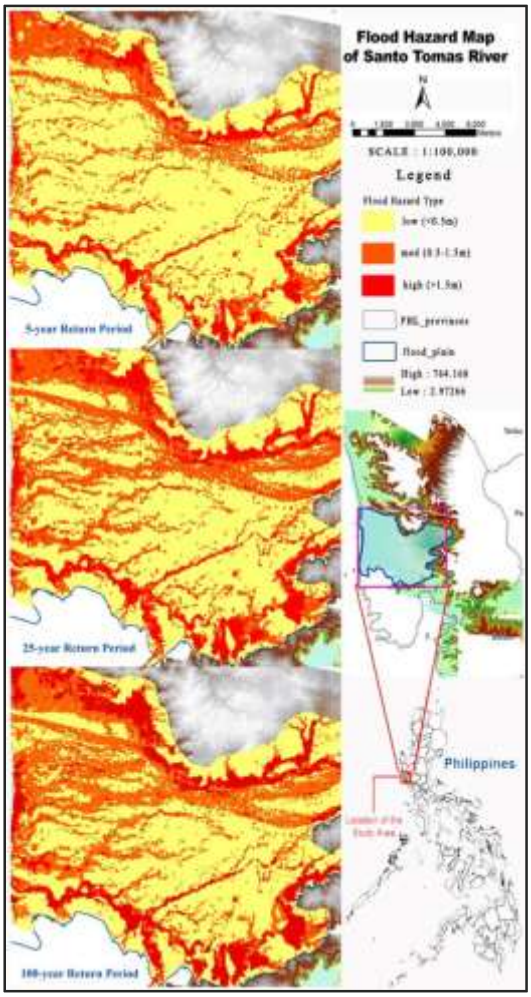

Figure 4: The flood hazard maps of Santo Tomas River at varying rainfall return periods.

2.5. Buildings Exposure and Vulnerability Assessment

GIS overlay analysis of the 3D building GIS data base and flood hazard maps for the Santo Tomas river basin was conducted to identify the exposure of buildings to various levels (low, medium, high) of flood hazards. For the determination vulnerability of buildings in the flood plains of the River basin, the degree exposure of buildings to flood was characterized with the comparison of building height and simulated flood depths. If the flood depth is less than 0.10 percent of the building's height, then it was coded as "Not vulnerable". If the flood depth is 0.10 to less than 0.30 of the building's height, then the vulnerability is "Low". On the other hand, if the flood depth is equal to 0.30 but less than 0.50, then the vulnerability is medium. If the flood depth is greater than or equal to 0.50 of the building's height, then the vulnerability is high.

3. Results and Discussion

3.1. GIS Buildings database

The extracted buildings as shown in Figure 5 were saved as GIS shape files. The number of extracted and attributed buildings according to the type are presented in Figure 6 where a total of 40, 838 equivalent to more than ninety six percent (96.83%) were identified as residential buildings and the remaining 1,335 equivalent to three percent (3.17%) are the other building types.

Figure 5: The extracted building footprints in the flood plains of Santo Tomas River.

3.2. Exposure of Buildings to Flood Hazard

The statistics generated as a result of the study, show that the number of buildings affected by flooding increases as the rainfall return period also increases. Majority of the buildings appeared to be flooded in all considered rainfall scenarios. This result might be due to the reason that the riverbed

ISSN: 1832-5505
Vol-2 Issue-01 Jan 2014

of the Santo Tomas River is higher than the ground level by 6.7 m (maximum) or 1.9 m (average) on the left bank side. On the right bank side, the riverbed is higher than the ground level by 2.4 m (maximum) or 0.5 m (average) as of May 2002 due to the lahar deposits from the Mount Pinatubo 1991 eruption (DPWH, 2003). Figure 7 shows the total number of buildings exposed to flood hazard at different rainfall return periods.

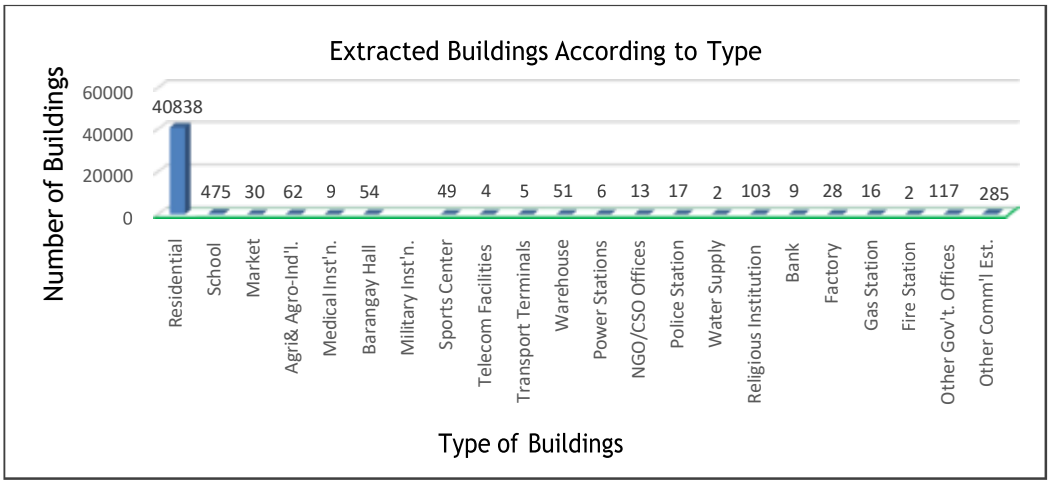

Figure 6: Extracted buildings with attributes in Santo Tomas River flood plain according to type.

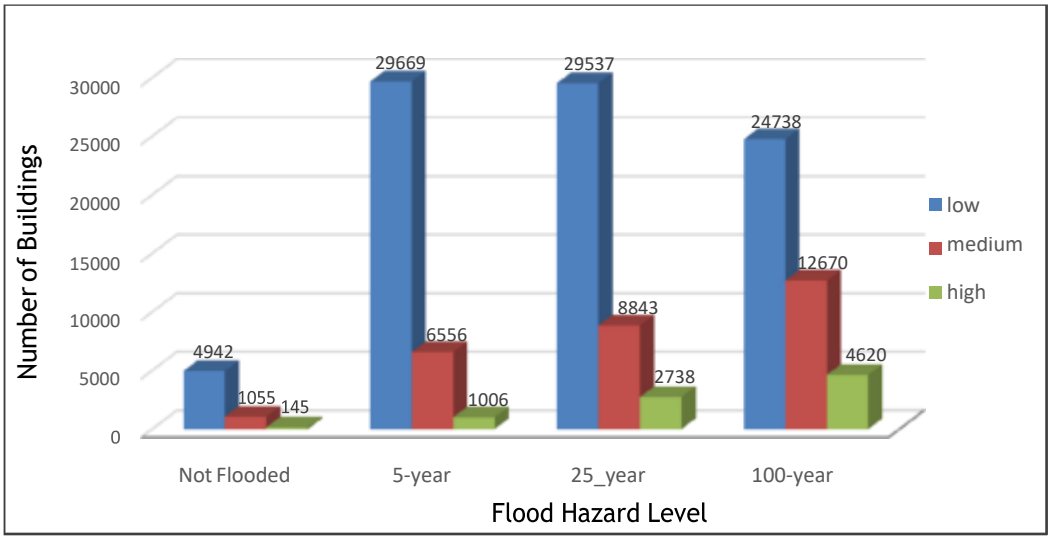

Figure 7: The number of buildings exposed to different hazard levels at varying rainfall return periods.

Among the flood-affected buildings, more number of buildings are exposed to low flood hazard levels than those in medium and high hazard levels. A total of 70.35 percent, 15.54 percent and 2.38 percent of the total buildings exposed at 5-year rainfall return period and 70.04%, 20.97% and 6.49% of the total buildings exposed at 25-year rainfall return period and 58.66%, 30.04% and 10.95% of the total buildings exposed at 100-year rainfall return period were at low, medium and high hazard levels, respectively. Consequently, the total number of buildings at 5-year medium hazard levels increased to 35 percent and 93 percent at 25-year and 100-year hazard levels, respectively, while

ISSN: 1832-5505
Vol-2 Issue-01 Jan 2014

the number of buildings exposed to 5-year high hazard was increased to 172 percent and 360 percent at 25-year and 100-year hazard levels, respectively. Majority of areas in the flood plain of the river basin where buildings are located are relatively prone to flooding, which also means of high hazard level where many lives and properties are at risk in an instance of flooding. The locations of these exposed buildings at varying rainfall return periods are presented in Figure 8, Figure 9 and Figure 10 at 5-year, 25-year an 100-year rainfall return periods, respectively. Figure 11 shows the number of buildings according to type that are exposed to flood hazard at different rainfall return periods.

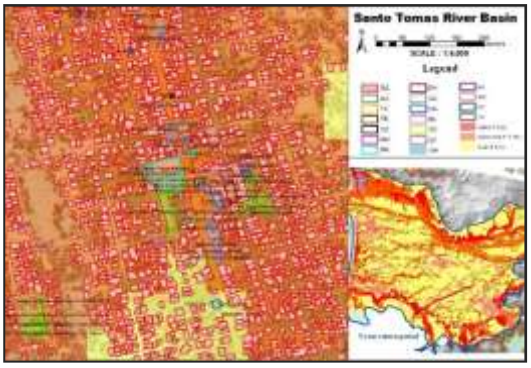

Figure 8: Location of buildings exposed to flood hazard at 5-year return period of rainfall events.

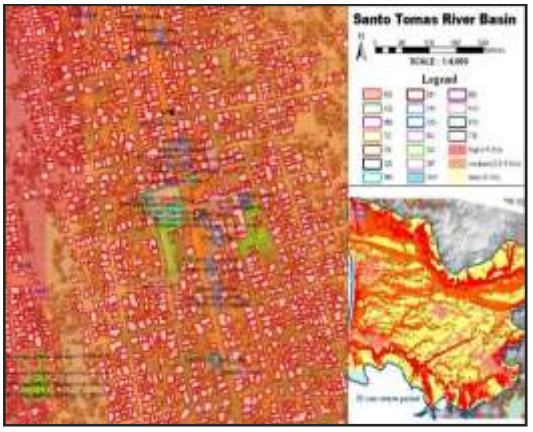

Figure 9: Location of buildings exposed to flood hazard at 25-year return period of rainfall events.

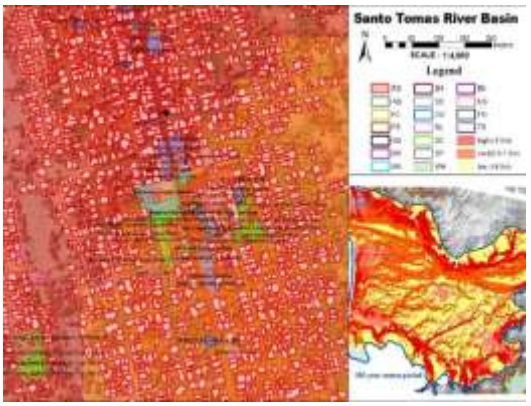

Figure 10: Location of buildings exposed to flood hazard at 100-year return period of rainfall events.

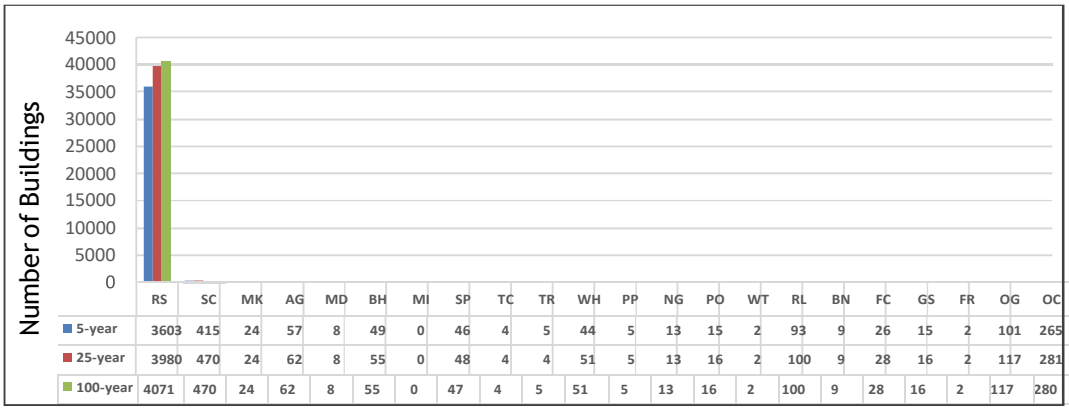

	RS	SC	MK	AG	MD	BH	MI	SP	TC	TR	WH	PP	NG	PO	WT	RL	BN	FC	GS	FR	OG	OC
5-year	3603	415	24	57	8	49	0	46	4	5	44	5	13	15	2	93	9	26	15	2	101	265
25-year	3980	470	24	62	8	55	0	48	4	4	51	5	13	16	2	100	9	28	16	2	117	281
100-year	4071	470	24	62	8	55	0	47	4	5	51	5	13	16	2	100	9	28	16	2	117	280

Figure 11: The number of buildings exposed to flood hazard according to type at varying return periods.

3.3. Vulnerability of Buildings to Flood Hazard

Statistics of the height of buildings and simulated flood depths comparison show that the number of buildings vulnerable to flooding increases as the rainfall return period increases and the vulnerable buildings are equivalent to 30 percent, 53

ISSN: 1832-5505
Vol-2 Issue-01 Jan 2014

percent and 61 percent of the buildings exposed to flooding at 5-year, 25-year and 100-year return periods, respectively. Figure 10 displays the total number of buildings vulnerable to flood hazard at different rainfall return periods.

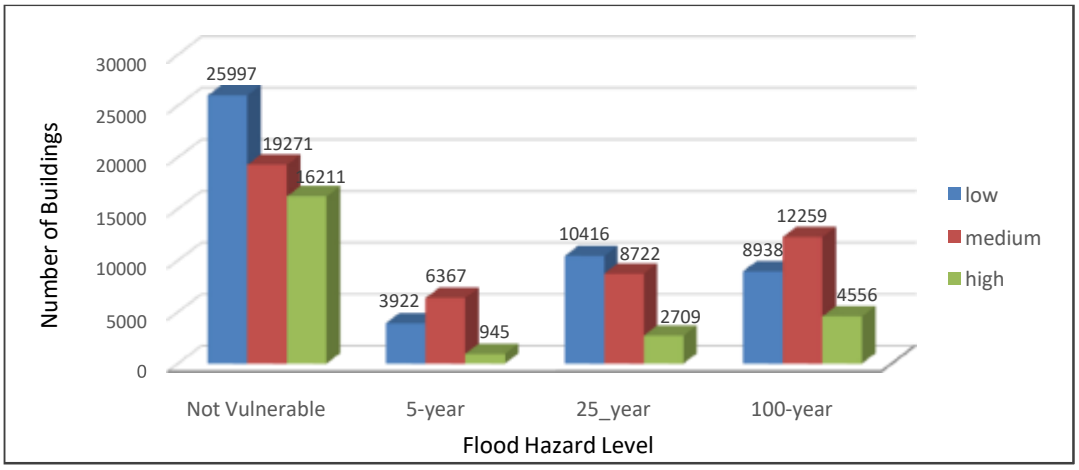

Figure 12: The number of buildings vulnerable to flood in terms of height at different hazard levels.

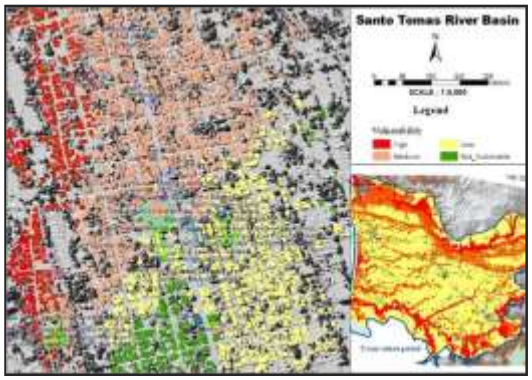

Figure 13: Location of buildings vulnerable to flood hazard at 5-year rainfall return period.

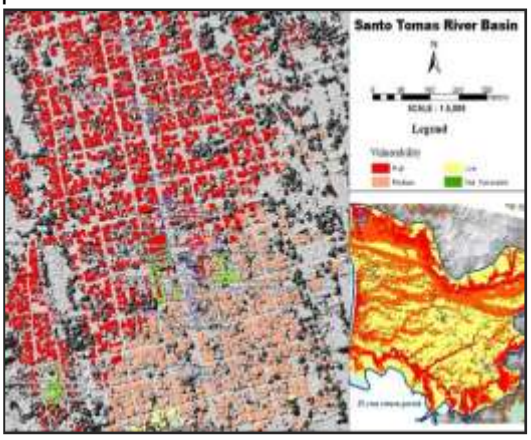

Figure 14: Location of buildings vulnerable to flood hazard at 25-year rainfall return period.

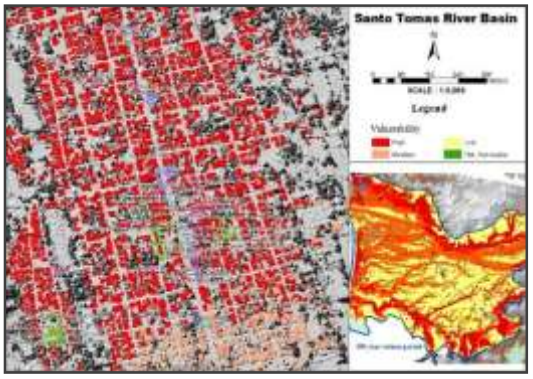

Figure 15: Location of buildings vulnerable to flood hazard at 100-year rainfall return period.

Based on the graphs in Figure 12, buildings under medium hazard are highest in number followed by buildings under low hazard. Comparing the results of buildings exposed and buildings vulnerable to flooding, most of the buildings exposed to medium and high hazard are vulnerable to flooding with an equivalent of 98.6% and 96.8% for medium hazard and 98.9% and 98.6% for high hazard at 25-year and 100-year return period, respectively, which implies a high rate of risk in times of flooding. However, all results for the vulnerability assessment of buildings were based on height and the other factors

ISSN: 1832-5505
Vol-2 Issue-01 Jan 2014

and engineering parameters such as structural components were not considered. The locations of these vulnerable buildings at varying rainfall return periods are presented in Figure 13, Figure 14 and Figure 15 at 5-year, 25-year an 100-year rainfall return periods, respectively. Figure 16 shows the number of vulnerable buildings according to type at different rainfall return periods.

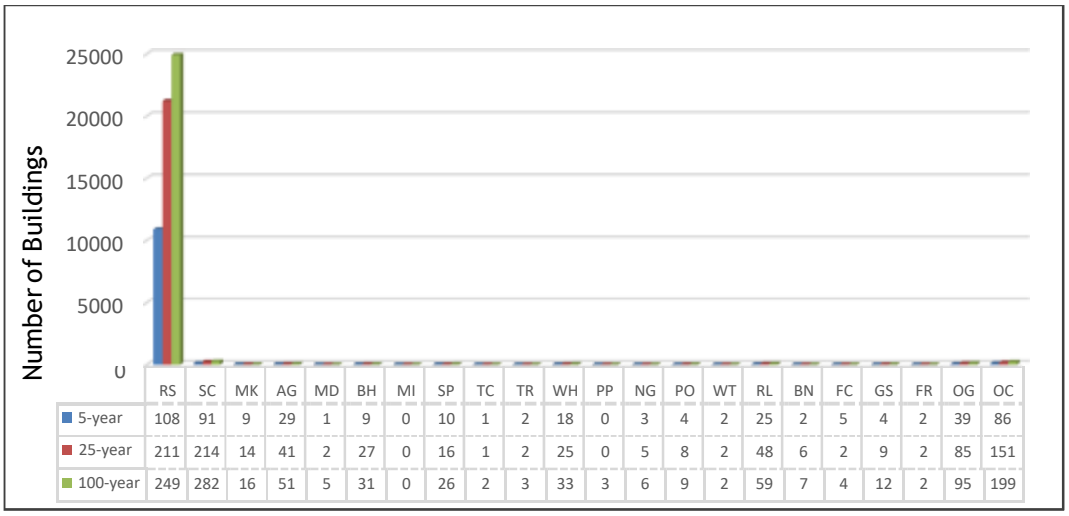

	RS	SC	MK	AG	MD	BH	MI	SP	TC	TR	WH	PP	NG	PO	WT	RL	BN	FC	GS	FR	OG	OC
5-year	108	91	9	29	1	9	0	10	1	2	18	0	3	4	2	25	2	5	4	2	39	86
25-year	211	214	14	41	2	27	0	16	1	2	25	0	5	8	2	48	6	2	9	2	85	151
100-year	249	282	16	51	5	31	0	26	2	3	33	3	6	9	2	59	7	4	12	2	95	199

Figure 16: The number of buildings vulnerable to flood hazard according to type at varying return periods.

4. Conclusion and Recommendations

The 3D building GIS database of Santo Tomas river basin was generated with the integrated modern LiDAR technology and Geographic Information System software. The buildings identified and attributed had a total number of 42,173 consisting of 96.83 % residential buildings and 3.17% other building types such as government and privately owned buildings. The building database and flood hazard maps used for the GIS overlay analysis produced a series of building exposure and vulnerability maps corresponding to the 5-year, 25-year and 100-year return period rainfall events.

Although the vulnerability assessment was only based on the building height, yet it can be very useful and informative for the community in the areas where the building locations were identified to be exposed and vulnerable to flooding. The statistics and maps generated during the course of this study are valuable pieces of information to the residents and local officials indicating identified possible risk when a particular rainfall event of specific return period is expected to occur. Furthermore, the locations of the buildings exposed and vulnerable to flooding can be used in undertaking appropriate measures for the possible flood disaster management to prevent or reduce loss of life, injury and other environmental consequences. Due to lack of other necessary data for the analysis during the course of this study, the analysis was only based on the height of the buildings extracted. It is recommended to expand the analysis where formal engineering decision analysis will be considered.

5. Acknowledgement

This work is an output of the Central Luzon State University (CLSU) Phil-LiDAR 1 project entitled "LiDAR Data Processing and Validation in Luzon: Region III and Pangasinan (Region I)" under the "PHIL-

ISSN: 1832-5505
Vol-2 Issue-01 Jan 2014

LiDAR 1 program "Hazard Assessment of 2/3 of the Philippines using LiDAR". The authors would like to extend sincere gratitude to the Department of Science and Technology (DOST) for the funding assistance and to the monitoring agency, the Department of Science and Technology – Philippine Council for Industry, Energy and Emerging Technology Research and Development (DOST-PCIEERD). Moreover, heartfelt thanks is being conveyed to the University of the Philippines Disaster Risk and Exposure for Mitigation (UP-DREAM)/Phil -LiDAR 1 Program research team for the provision of the Digital Elevation Models (DEMs) that were used in the project.

Reference

Awal, R., 2003. Application of Steady and Unsteady Flow Model and GIS for Floodplain Analysis and Risk Mapping: A Case Study of Lakhandei River, Nepal. (M. Sc. Thesis), Water Resources Engineering, IOE, Tribhuvan University, Kathmandu.

DENR, 2008. DAO No. 05 Series of 2008, Implementing Guidelines in the Preparation of Integrated Watershed Management Plan.

DPWH, 2003. The Study on Sabo and Flood Control for Western River Basins of Mount Pinatubo in the Republic of the Philippines: Final Report. Supporting Report. Appendix V-Inundation and Damage,p. v-3

Kron, W. and W. Willems. 2002. "Flood risk zoning and loss accumulation analysis for Germany." Proc. of the First InternationalConference on Flood Estimation. March 6-8, 2002. Berne, Switzerland.

Kron, W., 2005. Flood risk = Hazard _ Values _ Vulnerability. Water Int. 30, pp.58–68. Retrieved July 29, 2016, from citeseerx.ist.psu.edu

IPCC, 2012. In: Field, C.B., Barros, V., Stocker, T.F., Qin, D., Dokken, D.J., Ebi, K.L., Mastrandrea, M.D., Mach, K.J. (Eds.), Managing the Risks of Extreme Events and Disasters to Advance Climate Change Adaptation: Special Report of the Intergovernmental Panel on Climate Change. p. 582.

Raber, G.T., 2007. Impact of LiDAR Nominal Post Spacing on DEM Accuracy and Flood Zone Delineation. Photogrammetric Engineering and Remote Sensing 73, pp.793–804.

Rodolfo, K.S., and Umbal, J.V., 1992. Catastrophic Lahars on the West Flanks of Mount Pinatubo, Philippines: Proceedings of the Workshop on the Effects of Global Climate Change on Hydrology and Water Resources at the Catchment Scale, February 3-6, 1992, Tsukuba Science City, Japan, Japan-U.S. Committee on Hydrology, Water Resources, and Global Change, pp. 493-510.

Ruijin, M.., 2005. DEM Generation and Building Detection from Lidar Data. Photogrammetric Engineering and Remote Sensing, 71 (7), pp847-854.

Smith, K., and Ward, R., 1998. Floods: Physical Processes and Human Impacts, John Wiley and Sons, Chichester, USA.

ISSN: 1832-5505
Vol-2 Issue-01 Jan 2014

Tambunan, M., 2007. Flooding area in the Jakarta province on February 2 to 4 2007. Retrieved August 10, 2016, from http://a-a-r-s.org/aars/proceeding/ACRS2007/Papers/PS1.G5.2.pdf

UN/ISDR., 2005. Hyogo Framework for Action 2005e2015. Building the resilences of nations and communities to disasters.Retrieved August 1, 2016, from http://www.unisdr.org.

UN/ISDR., 2011b. Global Assessment Report on Disaster Risk Reduction. Geneva, Switzerland: United Nations. Retrieved July 28, 2016, from http://www. preventionweb.net/english/hyogo/gar/2011/en/home/ download.html

Yunfei, B., et al, 2007. Classification of LiDAR Point Cloud and Generation of DTM from LiDAR Height and Intensity Data in Forested Area, Retrieved August 10, 2016, from http://www.isprs.org/proceedings/XXXVII/congress/3b_pdf/63.pdf